Journal of Controlled Release 276 (2018) 157–167

Contents lists available at ScienceDirect

Journal of Controlled Release

journal homepage: www.elsevier.com/locate/jconrel

Formation of protein corona *in vivo* affects drug release from temperature-sensitive liposomes

Zahraa S. Al-Ahmady[1], Marilena Hadjidemetriou[1], James Gubbins, Kostas Kostarelos*

Nanomedicine Lab, Division of Pharmacy and Optometry, Faculty of Biology, Medicine and Health, University of Manchester, AV, Hill Building, Manchester M13 9PT, United Kingdom

ARTICLE INFO

Keywords:
Temperature-sensitive liposomes
Triggered release
Doxorubicin
Protein
Hyperthermia

ABSTRACT

Thermally triggered drug release from temperature-sensitive liposomes (TSL) holds great promise for cancer therapy. Different types of TSL have been designed recently for heat triggered drug release inside tumor blood vessels or after accumulation into the tumor interstitium. However, justification of drug release profiles is for far mainly based on *in vitro* release data. While these methods could be good enough to give early indication about the thermal sensitivity of TSL, they are still far from being optimum. This is because these methods do not take into consideration the actual adsorption of proteins onto the surface of TSL after their *in vivo* administration, also known as "protein corona" and the influence this could have on drug release. Therefore, in this study we compared thermal triggered drug release profile of two different types of doxorubicin encapsulated TSL; namely the lysolipid-containing TSL (LTSL) and traditional TSL (TTSL) after their *in vivo* recovery from the blood circulation of CD-1 mice. *Ex vivo* release profile at 42 °C was then tested either in the presence of full plasma or after removal of unbound plasma proteins (i.e. protein corona coated TSL). Our data showed that the influence of the environment on drug release profile was very much dependent on the type of TSL. LTSL release profile was consistently characterized by ultrafast drug release independent on the conditions tested. On the contrary, TTSL release profile changed significantly. Doxorubicin release from *in vivo* recovered TTSL was slow and incomplete in the presence of unbound plasma proteins, whereas very rapid drug release was detected from *in vivo* recovered and purified protein corona-coated TTSL in the absence of unbound proteins. Using mass spectrometry and quantification of protein adsorption, we confirmed that this discrepancy is due to the changes in protein adsorption onto TTSL when heated in the presence of unbound proteins leading to reduction in drug release. In summary this study showed that the formation of the *in vivo* corona on TSL will have a dramatic impact on their release profile and is dependent on both their lipid composition and the protein content of the environment in which drug release is triggered.

1. Introduction

Thermosensitive liposomes (TSL) represent a very promising "smart generation" of liposomal systems for targeted and triggered drug release in response to external mild hyperthermia. Following the pioneering work of Yatvin in the late 1970s [1], a lot of effort has been invested to explore the potential of TSL for cancer therapy. Indeed, over the past thirty years the development of TSL has been widely expanded starting from the molecular design of TSL all the way to clinical testing and determining their therapeutic aptitude [2]. Encapsulation of drug inside TSL, shields the body from the harmful effects of the drug when circulating in the blood stream. Once within the tumor, drug release from TSL can be tailored towards intravascular [3–7] or interstitial release [4,8] based on the timing between TSL administration and heat application. Generally, drug release from TSL is based on passive permeability through the lipid membrane when it passes through transition temperature (Tm). At body temperature the lipid membrane exists in solid phase only and therefore no release of hydrophilic drugs is expected. When TSL heated through their Tm, areas of the phospholipid molecules start to change from the solid (ordered) gel phase to the liquid (disordered) crystalline phase. This creates boundaries with packing defects between the two phases through which the drug permeability is enhanced [2,9]. In addition to that, lysolipids containing TSL mediate ultrafast drug release through the formation of lysolipids stabilized long lasting pores [10]. The release of encapsulated molecules is also affected by the loading mechanism. Significant difference

* Corresponding author.
E-mail address: kostas.kostarelos@manchester.ac.uk (K. Kostarelos).
[1] These authors contributed equally to the study

https://doi.org/10.1016/j.jconrel.2018.02.038
Received 2 November 2017; Received in revised form 8 February 2018; Accepted 26 February 2018
Available online 06 March 2018
0168-3659/

in the release rate of fluorescent dyes, such carboxyfluorescein (CF), was observed compared to doxorubicin (DOX) when tested under the same conditions. This difference is due to the collapse of the pH gradient mechanism used for DOX loading when the proton ions diffusion across the lipid membrane increases at Tm [11,12].

For a long time, the release profile from early types of TSL was misinterpreted as slow and incomplete under mild HT. Similarly, the relatively high Tm of this type of TSL (42–45 °C) suggested that high thermal dose, 1 h heating at temperature > 42 °C, is essential to achieve complete drug release. However, those assumptions were based on *in vitro* release data generated mainly in buffers and do not reflect the complexity of the physiological conditions [13–15]. It has been repeatedly reported that nanoparticles are spontaneously coated by proteins, once in contact with biofluids. Proteins adsorbed onto the surface of nanoparticles form a complex bioshell, known also as "protein corona", the composition of which is highly affected by the physicochemical characteristics of nanoparticles [16–19]. Protein corona formation has been previously investigated for different types of liposomes, however little is known about protein corona formation on TSL [20–24]. While the effect of protein corona on the cellular internalization [25], cytotoxicity [26,27] and targeting capability [28–30] have been so far explored in depth, the impact of protein corona on the release profile of active molecules from nanoparticles has not been systematically studied [31]. Most of the previous studies, as will be explained in more detail in the discussion, utilized *in vitro* drug release profile in the presence of plasma proteins to get early indication about the thermosensitive nature of TSL and the rate of drug release. However, these would not reflect the effect of actual protein adsorption under *in vivo* conditions.

In our previous studies, we developed a robust protocol, to investigate the *in vivo* protein corona formed onto clinically-used liposomes [23,24] and more recently onto gold nanoparticles [32] after their recovery from the blood circulation of mice. These studies demonstrated that the molecular complexity and morphology of the *in vivo* protein corona cannot be adequately predicted by the *in vitro* plasma incubation of NPs [23,24]. Even though the overall protein adsorption was found to be reduced by the functionalization of liposomes with PEG, it could not be fully suppressed [23,24]. Unlike previous work, in the present study, we investigated the role of protein corona on thermal triggered release of TSL after their *in vivo* recovery. In this way we can better simulate the actual protein adsorption profile compared to simple *in vitro* incubation (Fig. 1). *In vivo* protein coronas formed onto two different types of intravenously administered and doxorubicin-encapsulated TSL, namely traditional TSL (TTSL) and lysolipid-containing TSL (LTSL), were quantitatively and qualitatively characterized by mass spectrometry based proteomics. We hypothesized that TSL thermosensitivity is not only affected by the protein corona composition, but also by the environment in which the drug release is triggered. Therefore, we tested *ex-vivo* the release profile of doxorubicin from *in vivo* recovered corona-coated TSL (at 42 °C), in the presence of full plasma (in the presence of unbound proteins) and in buffer (i.e. protein corona coated TSL in the absence of unbound proteins).

2. Results

2.1. Physicochemical characterization of TSL before and after in vivo recovery

The physicochemical characteristics of TTSL and LTSL liposome systems employed in this study are summarized in Fig. 2 and Supporting table 1. Dynamic light scattering (DLS), ζ-potential measurements and negative stain transmission electron microscopy (TEM) were performed prior to the *in vivo* administration to analyse the properties and morphology of TSL in the absence of protein adsorption. TTSL and LTSL liposome systems had a mean hydrodynamic diameter between 120 and 130 nm and a negative surface charge of 25–30 mV. All liposomal formulations displayed low polydispersity values (< 0.07) indicating a narrow size distribution. TEM imaging showed well-dispersed, round shaped vesicles and their size correlating that of DLS measurements (Fig. 2C).

To investigate *in vivo* protein corona formation, TTSL and LTSL were intravenously injected and recovered from the blood circulation of CD-1 mice by cardiac puncture (Fig. 1). We have previously shown that a complex protein corona is formed as early as 10 min post-injection [24]. Our previous time evolution data demonstrated that despite the highly dynamic protein binding kinetics, protein corona formed onto PEGylated liposomal doxorubicin does not quantitatively change overtime [23]. In addition to that, our previous pharmacokinetics studies with TTSL and LTSL showed that approximately 60–70% of the injected TSL is still in the circulation 10 min post-injection which allows maximum liposomes recovery [6]. For the above reasons in this study we chose to investigate *in vivo* protein corona formation 10 minutes post-injection. A protocol combining size exclusion chromatography and membrane ultrafiltration was used for the isolation of corona-coated TSL from unbound and loosely bound plasma proteins, as we have previously described [23,24]. To characterize protein coronas formed *in vivo* (at 37 °C), liposomes were immediately purified from unbound proteins after intravenous administration, while to investigate the effect of mild HT on the formation of protein corona, *in vivo* recovered plasma (containing TSL liposomes) was incubated at 42 °C for 1 h, prior to the purification of corona-coated liposomes (Fig. 1C).

The physicochemical properties of the *in vivo* recovered protein-coated TSL with and without prior heating at 42 °C are shown in Fig. 2. Dynamic light scattering measurements of corona-coated TSL demonstrated that their size distribution broadened (larger polydispersity index), while their surface charge remained negative, both at 37 °C and 42 °C. In agreement with our previous studies investigating liposomal protein corona formation, we observed a blood-induced reduction in the mean diameter of liposomes, attributed to their high elastic structure [23,24]. This "shrinkage effect" was much more pronounced when corona-coated liposomes were exposed to mild hyperthermia (Table S1). In terms of structural integrity and morphology, TEM images revealed well-dispersed liposomes that retained their structural integrity after *in vivo* recovery, while the adsorption of proteins onto their surfaces was clearly evident. *Ex-vivo* heating (at 42 °C) of the *in vivo* recovered TTSL did not seem to affect their shape, whereas morphological changes towards elongated vesicles were observed in the case of LTSL. The structural differences observed between TTSL and LTSL after hyperthermia could be explained by their different lipid composition and especially their unique thermal responsive components [33,34]. LTSL are considered to be less robust compared to TTSL as no cholesterol is included in their design, in addition to the inclusion of 10 mol% of lysolipids that leads to pores formation after heating at 42 °C [34,35].

Having studied TSL surface properties and morphology, TSL systems stability and thermal responsiveness were initially evaluated *in vitro* by studying the release of doxorubicin (DOX) from the liposomes at 37 °C and 42 °C, respectively. In agreement with our previous findings [6], TTSL liposomal system showed very good drug retention capability after their *in vitro* incubation in full plasma at 37 °C (< 10% DOX leakage in 24 h). LTSL system on the other hand, exhibited short drug retention window of < 2 h (Fig. S1A). Thermal triggered drug release from TSL (at 42 °C) was first evaluated using traditional *in vitro* release methods in buffer (Fig. 3A) and full plasma (Fig. 3B). As expected from the chemical design of these two liposomal systems, LTSL showed very fast and complete drug release compared to slower release profile from TTSL after incubation with plasma proteins (Fig. 3B). While, similar thermal drug release profile was observed when the *in vitro* release was performed in buffer in the case of LTSL, very limited DOX release was observed (< 10%) for TTSL system (Fig. 3A). The presence of plasma proteins clearly favoured the temperature sensitivity of TTSL, presumably by gaining access into the grain boundary of the lipid

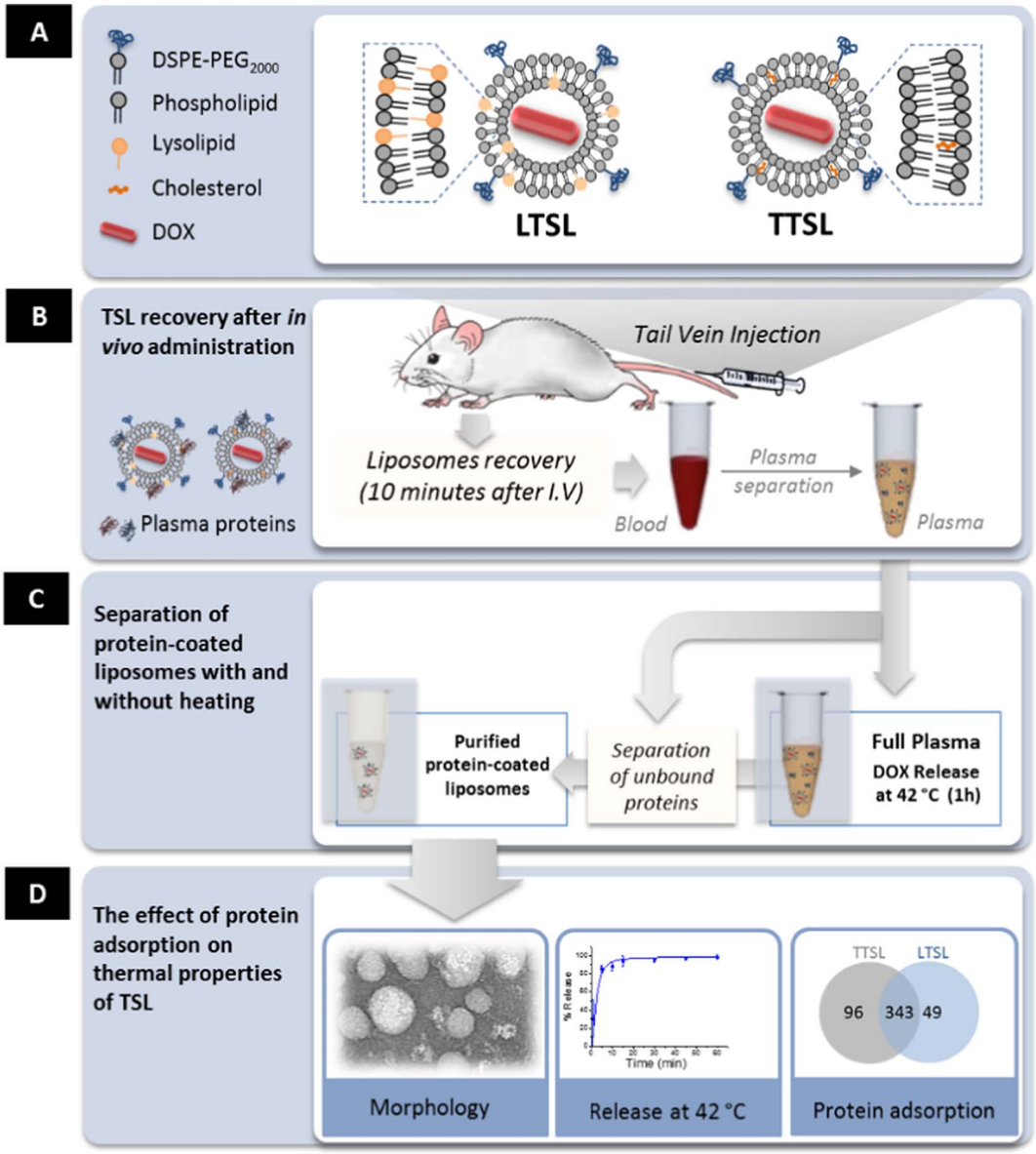

Fig. 1. Schematic description of the experimental design including;(A) Composition of different temperature sensitive liposomes (TSL) used in the study, namely lysolipids TSL (LTSL) and traditional TSL (TTSL);(B) *In vivo* protein corona formation after intravenous injection (i.v.) into tail vein (n = 3 CD-1 mice/group; 3 independent experiments replicated). Ten minutes after injection TSL were recovered from the blood by cardiac puncture and the plasma was then separated from the recovered blood by centrifugation; (C) Protein-coated TSL were purified from unbound proteins with and without *ex-vivo* heating at 42 °C for 1 h; (D) Protein-coated TSL were characterized in terms of morphology, thermal sensitivity and protein adsorption profile.

membrane at the transition temperature (Tm); (Fig. 3B).

Because of the significant role plasma proteins play on the thermal properties of some types of TSL and the fundamental differences in protein corona formation between *in vitro* and *in vivo* conditions, we studied thermal sensitivity of TSL after *in vivo* recovery from the blood circulation of CD1 mice. The percentage of DOX release at 42 °C was measured *ex vivo* in the presence and absence of unbound proteins (Fig. 3 C&D). Interestingly, as can be observed in Fig. 3C, purified corona-coated TTSL (in buffer), showed very fast and complete DOX release at 42 °C. TTSL thermal release in that case was almost identical to LTSL system. In contrast, *ex vivo* release at 42 °C from TTSL, in plasma, exhibited significantly slower drug release ($p < 0.05$). LTSL thermal triggered release on the other hand was still characterized by fast drug release even when heated in the presence of unbound proteins (Fig. 3D).

In order to understand the differences in the release profiles observed under the different conditions tested, we quantitatively and qualitatively characterized the *in vivo* protein corona formed onto the two different types of TSL. The amount of protein adsorbed was quantified by calculating the protein binding ability (Pb), defined as the amount of proteins associated with each μmol of lipid. Interestingly, we observed that the *in vivo* recovered LTSL adsorbed higher amount of protein than TTSL (Fig. 4A). In fact, compared to our previous studies [23,24], LTSL adsorb almost three times more proteins than Doxil-like non-temperature sensitive PEGylated liposome system [23,24]. This observation could be attributed to the difference in the fluidity of the phospholipid bilayers that can greatly influence the total amount of protein adsorbed.

In addition, protein adsorption profile after heating at 42 °C revealed a pronounced increase in the total amount of protein adsorbed for both, TTSL and LTSL (Fig. 4A). The increased amount of adsorbed proteins in the case of TTSL heated *ex-vivo* at 42 °C in the presence of

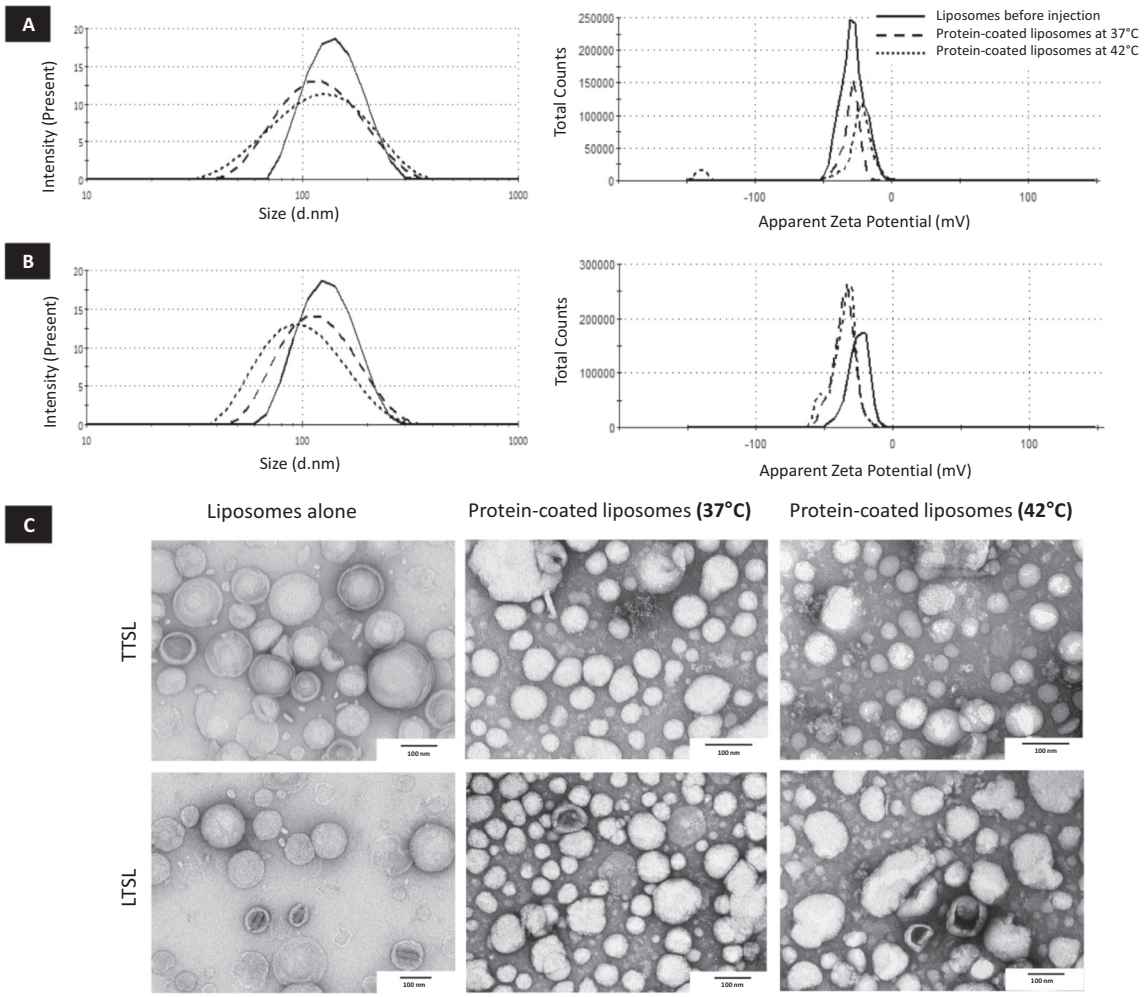

Fig. 2. The effect of protein corona formation on the physicochemical characteristics of TSL. Mean diameter (nm) and ζ-potential (mV) distributions are depicted for (A) TTSL and (B) LTSL liposome systems, before and after their interaction with CD-1 mouse plasma at 37 °C and 42 °C. The graphs are representative samples from three independent experiments. (C) Negative stain transmission electron microscopy images showing the morphological and structural characterization of LTSL and TTSL systems before and after protein corona formation at 37 °C and 42 °C. All scale bars are 100 nm.

free plasma proteins is most likely due to the increase in the bilayer fluidity. This change from the gel-phase into the liquid crystalline phase could facilitate the incorporation of more proteins into the phospholipid bilayers. These data explain the highly variable release profile observed from TTSL in the different conditions tested. TTSL liposomes released < 10% of encapsulated DOX when heated in buffer (Fig. 3A). This is expected and it is due to the chemical composition of TTSL. The rigid nature of TTSL due to the presence of cholesterol and HSPC lipids increases the Tm to 44 °C. Therefore, when heated at 42 °C very minimum release is detected, hence most of the lipid molecules are in a highly ordered state when not in interaction with plasma proteins. In comparison, complete and ultrafast release was observed from *in vivo* recovered protein-coated TTSL heated in buffer shown in Fig. 3C, which indicates that the interaction of plasma proteins with the lipid membrane is critical to facilitate drug release from the lipid bilayer during heating. It is important to stress here that the conditions tested in this case (Fig. 3C) are artificial lab conditions and may not directly reflect the *in vivo* scenario. On the other hand, heating TTSL in full plasma both *in vitro* and after *in vivo* recovery showed slow and incomplete release profile (Fig. 3B&D) which indicates that the increased adsorption of free protein in solution on TTSL surface during heating at 42 °C can act as a barrier to release. The release profile after heating in full plasma *in vitro* (Fig. 3B) was slightly faster than that detected from *in vivo* recovery (Fig. 3D). The differences in structural configuration and composition of *in vitro and in vivo* formed protein coronas, as we reported before [24], might explain such variability in the release profile.

The amount of adsorbed proteins on LTSL was also found to increase after heating at 42 °C in full plasma. Despite this increase, DOX release profile from LTSL did not significantly change in the presence and absence of unbound proteins (Fig. 3C&D). Complete drug release was observed from LTSL under both heating conditions tested, however, a slightly slower release was seen in the first 5 min when heated in the presence of unbound proteins. Based on these results, it seems that LTSL thermal release mechanism which depends on the long lasting pores formation by the lysolipids components is possibly still retained after 10 min of circulation *in vivo*.

This effect has been comprehensively investigated by Banno et al. [36], showing that the retention of lysolipids in LTSL is compromised. A rapid loss of lysolipid molecules from LTSL was observed within the first 10 min (from 9.6% to 3.6%) and this loss continued over time. However, the study showed that the thermosensitvity of LTSL was still retained despite such loss. In agreement with our release data, Banno et al. observed > 80% DOX release from LTSL recovered 10 min post-injection despite the rapid loss of lysolipid molecules. Therefore, this makes LTSL liposome system ideal for intravascular drug release (if heated shortly after injection), where heating occurs in excess of free plasma protein, compared to TTSL liposome system.

Proteins associated with TTSL and LTSL liposome systems at 37 °C

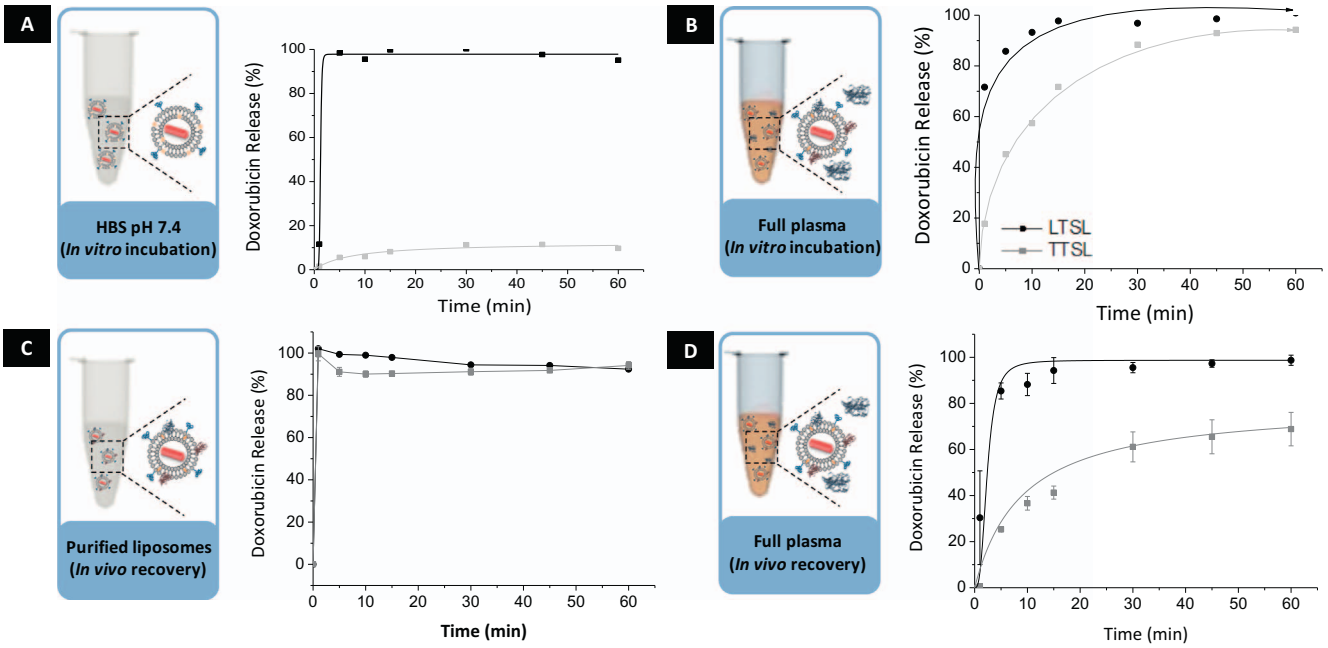

Fig. 3. Temperature sensitivity of TTSL and LTSL liposome systems after 1 h heating in a water bath at 42 °C. The percentage of doxorubicin release from TTSL and LTSL was measured; (A) after *in vitro* incubation in HBS buffer pH 7.4, (B) after *in vitro* incubation with full CD-1 mouse plasma, (C) from the *in vivo* recovered and purified liposomes (in the absence of unbound proteins) and (D) from the *in vivo* recovered liposomes in full plasma (before purification of unbound proteins). Statistical analysis of DOX release from TTSL from *in vivo* recovery in the presence and absence of unbound proteins using two-tailed unpaired student *t*-test revealed significant differences (p values < 0.05) at all time points tested.

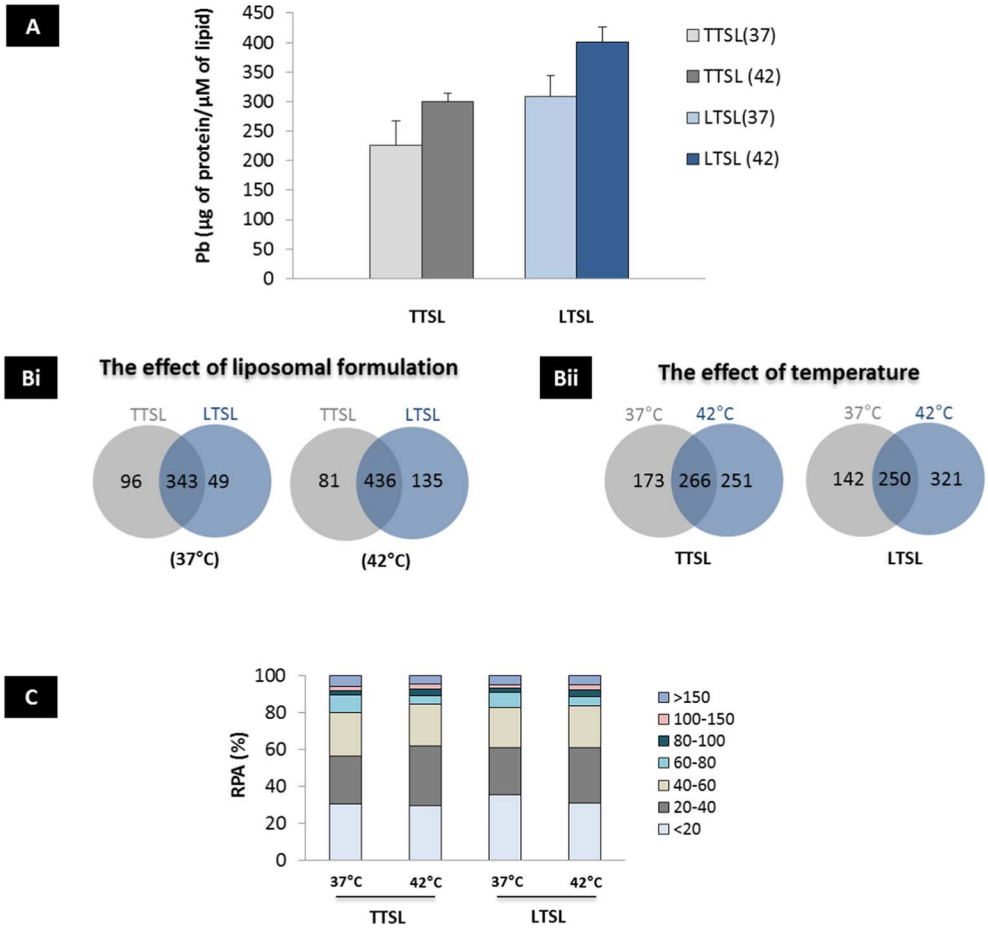

Fig. 4. Comparison of protein adsorption profiles onto TTSL and LTSL formed at 37 °C and 42 °C. (A) Comparison of the amount of proteins adsorbed onto TTSL and LTSL liposome systems. Pb values (µg of protein/µM lipid) represent the average and standard error from three independent experiments, each using three mice per liposome system; (Bi) Venn diagrams report the number of unique proteins identified in the 37 °C and 42 °C formed coronas on the two liposomal formulations tested and their respective overlap; (Bii) Venn diagrams illustrate the effect of temperature protein on corona formation for TTSL and LTSL; (C) Classification of the corona proteins identified according to their molecular mass.

A

37°C			
TTSL	RPA	LTSL	RPA
Apolipoprotein C-III	5.64 ± 1.09	Apolipoprotein C-III	6.38 ± 0.82
Apoe protein	4.93 ± 0.46	Beta-globin, A8DUK0 (+2)	5.72 ± 0.41
Beta-globin, A8DUK4	3.64 ± 1.03	Apoe protein	4.63 ± 0.41
Beta-globin, A8DUK0 (+2)	3.46 ± 1.13	Beta-globin, A8DUK4	4.03 ± 2.05
Beta-globin OS=Mus musculus castaneus	1.96 ± 1.00	Beta-2-globin (fragment)	3.35 ± 0.10
Beta-2-globin (fragment)	1.95 ± 0.47	Beta-globin OS=Mus musculus castaneus	2.60 ± 1.30
Alpha-2-macroglobulin	1.74 ± 0.29	Alpha-globin 1, Q91VB8 (+2)	2.54 ± 0.22
Alpha-globin 1, Q91VB8 (+2)	1.56 ± 0.32	Alpha-globin, A8DUV1	2.51 ± 0.10
Alpha-globin, A8DUV1	1.39 ± 0.17	Apolipoprotein E	1.68 ± 1.68
Ig mu chain C region	1.19 ± 0.13	Ig mu chain C region	1.46 ± 0.29
Apolipoprotein A-I	1.10 ± 0.19	Alpha-2-macroglobulin	1.41 ± 0.33
Apolipoprotein A-IV	1.05 ± 0.05	Protein Ighv7-1	1.04 ± 0.23
Protein Ighv7-1	0.93 ± 0.13	Apolipoprotein A-I	1.02 ± 0.14
Protein disulfide-isomerase	0.91 ± 0.07	Apolipoprotein A-IV	0.96 ± 0.17
Actin, cytoplasmic 1	0.90 ± 0.08	H-2 class I histocompatibility antigen, Q10 alpha chain	0.93 ± 0.04
78 kDa glucose-regulated protein	0.89 ± 0.09	Apolipoprotein C-IV	0.87 ± 0.06
Corticosteroid 11-beta-dehydrogenase isozyme 1	0.87 ± 0.12	Actin, cytoplasmic 1	0.85 ± 0.10
Apolipoprotein B-100	0.84 ± 0.08	Apolipoprotein B-100	0.80 ± 0.03
Membrane-associated progesterone receptor component 1	0.81 ± 0.10	Corticosteroid 11-beta-dehydrogenase isozyme 1	0.79 ± 0.04

B

42 °C			
TTSL	RPA	LTSL	RPA
Beta-globin, A8DUK0 (+2)	5.48 ± 1.81	Beta-globin, A8DUK0 (+2)	4.47 ± 0.54
Beta-globin, A8DUK4	4.62 ± 3.04	Beta-globin, A8DUK4	4.22 ± 0.65
Apoe protein	3.84 ± 0.22	Apolipoprotein C-III	2.81 ± 0.90
Beta-2-globin (fragment)	3.21 ± 0.53	Apoe protein	2.76 ± 0.57
Alpha-globin 1, Q91VB8 (+2)	2.79 ± 0.76	Alpha-globin 1, Q91VB8 (+2)	2.69 ± 0.18
Alpha-globin, A8DUV1	2.36 ± 0.80	Beta-2-globin (fragment)	2.37 ± 0.24
Mannose-binding protein C	1.44 ± 0.10	Mannose-binding protein C	1.48 ± 0.31
Argininosuccinate synthase	1.36 ± 0.19	Argininosuccinate synthase	1.42 ± 0.18
Apolipoprotein C-III	1.30 ± 0.65	Alpha-globin, A8DUV1	1.42 ± 0.72
Apolipoprotein E	1.21 ± 1.21	Glyceraldehyde-3-phosphate dehydrogenase	1.31 ± 0.16
Alpha-enolase	1.13 ± 0.13	Alpha-2-macroglobulin	1.28 ± 0.27
Estradiol 17 beta-dehydrogenase 5	1.12 ± 0.07	Alpha-enolase	1.00 ± 0.09
Glyceraldehyde-3-phosphate dehydrogenase	1.10 ± 0.12	Estradiol 17 beta-dehydrogenase 5	0.93 ± 0.10
Alpha-2-macroglobulin	1.05 ± 0.02	Beta-globin OS=Mus musculus castaneus	0.93 ± 0.93
Beta-globin OS=Mus musculus castaneus	0.99 ± 0.99	Apolipoprotein A-I	0.90 ± 0.26
Vitronectin	0.89 ± 0.16	Ig mu chain C region	0.86 ± 0.24
Ig mu chain C region	0.85 ± 0.19	Protein Ighv7-1	0.84 ± 0.19
Antithrombin-III	0.85 ± 0.07	Alpha-2-HS-glycoprotein	0.83 ± 0.07
Apolipoprotein A-I	0.79 ± 0.15	Antithrombin-III	0.82 ± 0.11
Alpha-2-HS-glycoprotein	0.74 ± 0.21	Clusterin	0.72 ± 0.04

Fig. 5. Most-abundant proteins (top-20) identified adsorbed onto TTSL and LTSL systems after protein corona formation at (A) 37 °C and (B) 42 °C measured by LCMS/MS. Relative protein abundance (RPA) values represent the average and standard error from three independent experiments, each using 3–4 mice.

and 42 °C were separated by SDS-PAGE and visualized with EZ Blue staining (Fig. S2). In agreement with protein quantification results, LTSL were found to adsorb the highest amount of proteins which further increased at 42 °C.

A comprehensive identification of proteins associated with TSL at 37 °C and 42 °C was performed by mass spectrometry. The Venn diagrams in Figure 4Bi illustrate the number of common and unique proteins adsorbed onto TTSL and LTSL at 37 °C and 42 °C. The majority of proteins identified were common between TTSL and LTSL both at 37 °C (n = 343) and at 42 °C (n = 436). However, the unique proteins identified (at both 37 and 42 °C) demonstrated that the difference in liposomal composition between TTSL and LTSL shapes protein corona formation, as previously shown by others [37]. Due to the tendency of lysolipid loss from LTSL, protein adsorption profile may change overtime and would certainly worth more investigation. The temperature was also found to greatly influence protein adsorption profiles (Figure 4Bii). Mahmoudi et al. have previously investigated the effect of temperature on protein corona formation. The *in vitro* incubation of superparamagnetic nanoparticles with protein solutions at different temperatures, ranging from 5 °C to 45 °C resulted in different degree of protein coverage and different corona composition [38]. In our study, hyperthermia was not only found to increase the total amount of protein adsorbed onto the surface of liposomes but also modified the composition of protein corona. The *ex vivo* heating of TTSL and LTSL at 42 °C was found to increase the complexity of protein corona, especially in the case of LTSL, where 321 unique proteins were identified. Our results also demonstrate that hyperthermia results in the replacement of some proteins (initially interacted with liposomes at 37 °C) by others. This is well illustrated by the 173 and 142 proteins, found on the surface of TTSL and LTSL respectively, only at 37 °C.

We have also classified the protein adsorption profile on TTSL and LTSL liposome systems based on the molecular weight of the proteins adsorbed. As illustrated in Fig. 4C, the majority of the bound proteins (> 85%) are of low molecular weight (MW < 80). This was in strong agreement with previous observations by us and others [23,26], that the protein adsorption tendency under dynamic conditions is towards low molecular weight. Very little fluctuation in the contribution of each protein group (classified based on MW) on the corona composition was observed between the two liposomes tested at 37 °C and 42 °C. This indicates that the formation of long lasting pores after LTSL heating at 42 °C [34] did not further enhance low molecular weight protein adsorption.

To better understand the protein corona formation onto TSL, we determined the relative protein abundance (RPA) of identified proteins. Fig. 1 summarizes the 20 most abundant proteins adsorbed onto *in vivo* recovered TTSL and LTSL before and after *ex vivo* heating. Apolipoproteins and immunoglobulins were the most abundant classes of corona proteins present in both conditions. RPA values demonstrated that for the two types of TSL tested the ranking of the most abundant proteins changed after *ex vivo* heating. For example, the RPA of Apolipoprotein C-III has dramatically decreased on both TTSL and LTSL after heating. Interestingly, albumin that is usually used as model protein to simulate the effect of protein adsorption on the release profile [39] was not identified in the top 20 proteins, both at 37 °C and 42 °C. This indicates the specificity of the interaction of TSL with plasma proteins, as our previous findings demonstrated that serum albumin is indeed in the top 20 proteins adsorbed onto *in vivo* recovered Doxil-like non-temperature sensitive PEGylated liposome system [23,24]. This also implies that the most abundant proteins in the plasma are not necessarily the most abundant corona proteins [23,24].

3. Discussion

Thermal triggered drug release from TSL, represents a very promising and rapidly evolving area in particular for cancer therapy [2]. Among the different triggering modality, mild hyperthermia, has provided to be one of the most promising and well controlled triggering modalities and has already progressed towards clinical evaluation [40–42]. The success of this smart delivery approach depends on achieving the desirable balance between minimising drug leakage at body temperature and maximizing drug release in the heated tumor [8]. Based on that, *in vitro* testing of drug release rate at body temperature and mild hyperthermia range (41–43 °C), has always been considered a prerequisite for early prediction of the therapeutic effectiveness of TSL [5,6,43–45]. However, the weakness of these traditional techniques is that the performance of TSL *in vitro* cannot directly predict their behaviour under the complex *in vivo* conditions. Koning and coworkers have depicted recently the different factors that can influence the performance of TSL with the aim to get more understanding about the extent that *in vitro* testing can be translated into *in vivo* therapeutic effect. These factors include; the TSL blood kinetics, the timing between injection and HT, duration of HT and the tumor vascularisation [46].

One of the most important and instant factor is the change in surface properties of TSL once in the blood stream as a result of plasma protein adsorption. It is now well accepted that TSL behaviour is highly influenced by blood components in particular plasma proteins to variable degrees depending on the lipid composition [2,6,14,33,39]. PEGylation could increase blood circulation time and improve thermal properties of TSL, but was shown not to be able to prevent the interaction with plasma proteins [33,39]. Hossann et al. has recently attempted to identify the effect of individual plasma components that essentially affect the integrity and thermal sensitivity of TSL. In that particular study, the rate of drug release from different types of TSL was tested in the presence of albumin, immunoglobulin and lipoprotein since they represent the major protein components in human blood. The conclusion of that study was that individual serum proteins cannot predict the complex composition of full plasma, therefore, the use of plasma or serum were considered inevitable for evaluation of TSL stability and thermal sensitivity [39]. However, the effect of serum on the release profile can vary considerably with the origin of the serum used, its concentration and the duration of exposure. This can explain the discrepancy in the release data reported from different TSL systems [14,47]. The effect of plasma components on the thermal sensitivity of TSL can also justify the increase in therapeutic activity observed in a number of preclinical studies over a wide range of tumor models despite being considered of having slow and incomplete drug release using mild heating conditions (42 °C) *in vitro* [48]. This effect has been studied in details recently by Lokerse et al., where they compared four different types of TSL composed of DPPC:DSPC:DSPE-PEG_{2000} but with different proportions of DPPC:DSPC lipids. *In vitro* release data after 1 h heating at 42 °C revealed that drug release rate decrease with increasing DSPC lipid mol% and indeed cryo-TEM images of liposomes at DPPC:DSPC 50:50 mol% confirmed that most of those liposomes were filled with DOX crystals which verify the slow and incomplete release profile. Those differences in release profile were less apparent *in vivo*, using intravital microscopy. Moreover, a burst effect was observed which was unexpected based on *in vitro* testing which again confirm the limitation of *in vitro* testing to predict therapeutic effectiveness [46] Fig. 5.

Similar findings were reported before by Li et al. using real-time imaging. Efficient intravascular DOX release after heating at 42 °C was observed followed by rapid uptake of DOX by endothelial cells and tumor cells. This resulted in high and homogeneous DOX penetration into tumor cells and improved tumor growth control [11]. Li observations are in a good agreement with Manzoor et al. observations showing rapid intravascular release from LTSL followed by extravasation into tumor tissue [3].

Similarly, biomolecular adsorption can influence the drug retention and *in vivo* behaviour of other types of nanocarriers. Peng et al. has illustrated that pre-exposure of polymeric nanocarriers (loaded with coumarin-6) to bovine serum albumin reduce the drug release rate and has significant impact on *in vivo* behaviour (prolonged blood circulation

time and changed organs distribution profile) [49]. Protein corona can also reduce burst release effect observed with protein conjugated nanocarrier (e.g. Abraxane) and surface-loaded nanocarrier (e.g. iron oxide nanoparticles) [50]. The observed decrease in drug release in those studies became more evident in the presence of unbound proteins, presumably because this will be associated with additional shielding effect [50]. Although those studies concerned with drug release at body temperature, it agrees with our findings that heat triggered drug release from TTSL was slow and incomplete when tested in the presence of unbound plasma proteins.

In addition to the effect of protein corona on drug release properties, recent efforts have illustrated that protein corona layering around nanoparticles can act as a reservoir with high payload capacity for therapeutic molecules such as anticancer drugs or genetic materials [51,52]. The release of protein corona loaded drugs can be controlled in different ways utilising the properties of the core NP. An interesting example on that is using thermal triggered release of DOX incorporated into protein corona layer around gold nanorods (GNR). Upon exposure to external laser, incorporated DOX was released, possibility due to the restructuring process of protein corona as a result of protein denaturation in the proximity of GNR [52].

Our findings illustrated that the interaction of plasma proteins with TSL changed after heating and is affected by many parameters, such as the lipid composition of TSL and temperature. The variability of the protein adsorption has a clear influence on the real thermosensitivity and drug release profile observed. This observation was supported for the first time with morphological data that illustrated a very clear change in protein corona layer on TSL when heated in the presence of unbound proteins. Furthermore, we provided a comprehensive analysis of protein corona composition using mass spectroscopy. This illustrated that testing drug release by simple *in vitro* incubation is of limited value to predict the complex liposomal-protein interactions *in vivo* and the influences those can have on thermal triggered release.

Over the past few years, several TSL systems have been designed to trigger drug release either intravenously, while still in the blood stream, or after accumulation into the tumor interstitium. As the protein species will differ significantly between the blood and tumor, the change in the release environment should be carefully considered. To put this into a clinical context, our findings will have a greater impact on the critical evaluation of TSL and iterate on the necessity to take into account the different parameters that can affect drug release. In phase III clinical trial of ThermoDOX® in combination with radiofrequency ablation (RFA) for hepatocellular carcinoma, initial data showed that the treatment did not meet the expected therapeutic efficacy compared to RFA control group. However, a recent meta-analysis of the data revealed 58% improved overall survival in a subgroup of patients who received optimized RFA for at least 45 minutes. It is highly believed now that the timing and duration of heating may be the critical factors behinds ThermoDOX® clinical trial data, in addition to other peripheral hurdles that were experienced in some clinical centres [53,54].

Taking all the above into consideration, it is evident that further systematic preclinical and clinical studies are required to offer insight into the best combination of TSL and HT protocol applied taken into consideration the chemical design of TSL and the complexity of the *in vivo* environment where the actual heat-triggered release will take place.

4. Conclusion

Our findings demonstrated the interaction of plasma proteins with TSL is a highly variable process and is affected by many parameters. The variability of the protein adsorption has a clear influence on the real thermosensitivity and drug release profile observed. This effect was very much dependent on the lipid composition of the liposomes tested and was not predictable. Using mass spectrometry and quantification of protein adsorption, we confirmed that the discrepancy in heat-triggered profile is due to the changes in protein adsorption. This illustrated that testing drug release by simple *in vitro* incubation is of limited value to predict the complex liposomal-protein interactions *in vivo* and their impact on thermal triggered release. In summary, this study has shown that thermal triggered release from TSL formulations cannot be predicted solely based on their chemical composition and on *in vitro* release studies and the environment of drug release under realistic *in vivo* conditions should be taken into account.

5. Experimental

5.1. Materials

Dipalmitoylphosphatidylcholine (DPPC); monostearoyl phosphatidylcholine (MSPC); hydrogenated soy phosphatidylcholine (HSPC); 1,2-distearoyl-sn-glycero-3-phosphoethanolamine-*N*-[methoxy(polyethylene glycol)-2000] (ammonium salt) (DSPE-PEG2000) were purchased from Lipoid GmbH (Germany). Cholesterol, chloroform, methanol, 4-(2-Hydroxyethyl)piperazine-1-ethanesulfonic acid (HEPES), and doxorubicin hydrochloride (Dox) were purchased from Sigma (UK). All chemical substances and solvents were used without further purification.

5.1.1. Liposome preparation and DOX encapsulation

Two different types of TSL (TTSL and) were prepared by a thin lipid film hydration method followed by extrusion as described previously. Table S1 shows the liposomal formulation employed, the lipid composition and the molar ratios. Briefly, lipids were dissolved in chloroform:methanol mixture (4:1) in a round bottom flask and the organic solvents were then evaporated using a rotary evaporator to produce dried lipid films. Lipid films were then hydrated with ammonium sulphate 250 mM (pH 8.5) at 60 °C and small unilamellar liposomes were produced by extrusion through 800 nm and 200 nm extrusion filters (Whatman, VWR, UK) 5 times each then 10 times through 100 nm filters (Whatman, VWR, UK) using a mini-Extruder (Avanti Polar Lipids, Alabaster, AL). Liposome size and surface charge were measured by using Zetasizer Nano ZS (Malvern, UK).

Doxorubicin (DOX), an anticancer drug, was loaded into TSL by the ammonium sulphate gradient method. First, external buffer was exchanged by passing the liposomes through Sepharose CL-4B gel filtration column equilibrated with HBS buffer, then incubated with DOX at 1:20 DOX/Lipid mass ratio at 37 °C for LTSL (1.5 h) or at 39 °C for TTSL (5 h). After incubation, liposomes were passed through PD-10 desalting columns (GE Healthcare Life Sciences) to remove any free DOX. Encapsulation efficiency (% EE) was calculated by comparing the total fluorescence intensity of DOX post and pre gel filtration.

% EE = I(t) post column/I(t) pre column *100.

Where, I(t) is the total fluorescence intensity of the liposome suspension after adding 2 μl Triton X-100 (10% in HBS, pH 7.4).

5.1.2. Animal experiments

Eight to ten week old female CD1 mice were purchased from Charles River (UK).Animal procedures were performed in compliance with the UK Home Office Code of Practice for the Housing and Care of Animals used in Scientific Procedures. Mice were housed in groups of five with free access to water and kept at temperature of 19–22 °C and relative humidity of 45–65%. Before performing the procedures, animals where acclimatized to the environment for at least 7 days.

5.1.3. TSL recovery after in vivo administration

CD1 mice were anesthetized by inhalation of isoflurane and TSL were administered intravenously via the lateral tail vein, at a lipid dose of 0.125 mM/g body weight to achieve a final doxorubicin dose of 5 mg/kg body weight, used for preclinical studies [5,7,35] 10 min post-injection, blood was recovered by cardiac puncture using K2EDTA coated blood collection tubes. Approximately 0.5-1 ml of blood was

recovered from each mouse. Plasma was prepared by inverting 10 times the collection tubes to ensure mixing of blood with EDTA and subsequent centrifugation for 12 min at 1300 RCF at 4 °C. Supernatant was collected into Protein LoBind Eppendorf Tubes and the plasma samples obtained from three mice were pooled together for a final plasma volume of 1 ml. Three experimental replicates were performed and therefore 9 mice were used in total for each time point.

5.1.4. Serum stability and temperature sensitivity of liposomes

In vitro release experiments were performed at 37 °C and 42 °C in full CD-1 mouse serum prepared by collecting 0.5–1 ml of blood by cardiac puncture from each mouse using K2EDTA coated blood collection tubes. Blood samples were inverted 10 times to ensure proper mixing of blood with EDTA followed by subsequent centrifugation for 12 min at 1300 RCF at 4 °C. Release studies experiments performed with TSL recovered after *in vivo* administration were done either directly after recovery (in full plasma in the presence of free unbound plasma proteins) or after separation of protein-coated liposomes from unbound and weakly bound proteins.

At different time points 10 μl samples were withdrawn and further diluted to 200 μL with HBS (pH 7.4) and measured at 480 nm excitation wavelength and 593 nm emission wavelength (slit 10/20 nm) in a quartz cuvette using Cary Eclipse Fluorescence Spectrophotometer (Agilent Technologies). The intensity of the fluorescence signals was then normalized and the % of Dox release was calculated as; Dox release % = [I(s) − I(0)]/[I(t) − I(0)], where I(s) is the fluorescence intensity of individual samples at different time points, I(0)is the background fluorescence intensity of liposome samples after purification and I(t)is the fluorescence intensity of liposomes suspension after lysis with 3 μl of 1% Triton X-100 in HBS followed by heating at 42 °C for 20 min.

5.1.5. Separation of protein-coated liposomes from unbound and weakly bound proteins

TTSL and LTSL liposome systems recovered from *in vivo* experiments were separated form excess plasma proteins by size exclusion chromatography followed by membrane ultrafiltration, as we have previously described [24]. This process has been done wither immediately after the *in vivo* incubations (Protein-coated liposomes at 37 °C) or after 1 h *ex-vivo* heating at 42 °C (Protein-coated liposomes at 42 °C). In both cases 1 ml of plasma samples containing *in vivo* recovered liposomes with and without heating at 42 °C was loaded onto a Sepharose CL-4B (SIGMA-ALDRICH) column (15 × 1.5 cm) equilibrated with HBS. Chromatographic fractions 4,5 and 6 containing liposomes were then pooled together and concentrated to 500 μl by centrifugation using Vivaspin 6 column (10,000 MWCO, Sartorious, Fisher Scientific) at 3000 rpm. Vivaspin 500 centrifugal concentrator (1,000,000 MWCO, Sartorious, Fisher Scientific) was then used at 3000 rpm, to further concentrate the samples to 100 μl and to ensure separation of protein-coated liposomes from the remaining large unbound proteins. Liposomes were then washed 3 times with 100 μl HBS to remove weekly bound proteins.

Please note that the procedures of liposomes purification with Sepharose CL-4B and Vivaspin has no impact on liposomes size and DPI. These are routinely used procedures for DOX encapsulation (table S1).

5.1.6. Size and zeta potential measurements using dynamic light scattering (DLS)

After incubation of liposomes at different temperature for each condition tested, DLS measurements were performed at RT (25 °C). Liposome size and surface charge were measured using Zetasizer Nano ZS (Malvern, Instruments, UK). For size measurement, samples were diluted with distilled water in 1 ml cuvettes. Zeta potential was measured in disposable Zetasizer cuvettes and sample dilution was performed with distilled water. Size and zeta potential data were taken in three and five measurements, respectively.

5.1.7. Transmission electron microscopy (TEM)

TSL under different conditions tested were visualized with transmission electron microscopy (FEI Tecnai 12 BioTwin) before and after their *in vivo* interaction with plasma proteins at 37 °C and 42 °C. Samples were diluted to 1 mM lipid concentration, then a drop from each liposome suspension was placed onto a Carbon Film Mesh Copper Grid (CF400-Cu, Electron Microscopy Science) and the excess suspension was removed with a filter paper. Staining was performed using aqueous uranyl acetate solution 1%.

5.1.8. Quantification of adsorbed proteins

Proteins associated with recovered liposomes were quantified by BCA Protein assay kit. Pb values, expressed as μg of protein/μM lipid were then calculated and represented as the average ± standard error of three independent experiments. For the BCA assay, a 6-point standard curve was generated by serial dilutions of BSA in HBS, with the top standard at a concentration of 2 μg/ml. BCA reagent A and B were mixed at a ratio of 50:1 and 200 μl of the BCA mixture were dispensed into a 96-well plate, in duplicates. Then, 25 μl of each standard or unknown sample were added per well. The plate was incubated for 30 min at 37 °C, after which the absorbance was read at 574 nm on a plate reader (Fluostar Omega). Protein concentrations were calculated according to the standard curve. To quantify lipid concentration, 20 μl of each samples was mixed with 1 ml of chloroform and 500 μl of Stewart assay reagent in an Eppendorf tube. The samples were vortexed for 20 s followed by 1 minute of centrifugation at 13000 rpm. 200 μl of the chloroform phase was transferred to a quartz cuvette. The optical density was measured using Cary 50 Bio Spectrophotometer (Agilent Technologies) at 485 nm. Lipid concentration was calculated according to a standard curve.

5.1.9. Mass Spectrometry

Proteins associated with 0.05 μM of *in vivo* recovered TSL were mixed with Protein Solving Buffer (Fisher Scientific) for a final volume of 25 μl and boiled for 5 min at 90 °C. Samples were then loaded in 10% Precise Tris-HEPES Protein Gel (Thermo Scientific). The gel was run for 3–5 min 100 V, in 50 times diluted Tris-HEPES SDS Buffer (Thermo Scientific). Staining was performed with EZ Blue™ Gel Staining reagent (Sigma Life Science) overnight followed by washing in distilled water for 2 h. Bands of interest were excised from the gel and dehydrated using acetonitrile followed by vacuum centrifugation. Dried gel pieces were reduced with 10 mM dithiothreitol and alkylated with 55 mM iodoacetamide. Gel pieces were then washed alternately with 25 mM ammonium bicarbonate followed by acetonitrile. This was repeated, and the gel pieces dried by vacuum centrifugation. Samples were digested with trypsin overnight at 37 °C.

Digested samples were analysed by LC-MS/MS using an UltiMate® 3000 Rapid Separation LC (RSLC, Dionex Corporation, Sunnyvale, CA) coupled to Orbitrap Velos Pro (Thermo Fisher Scientific) mass spectrometer. Peptide mixtures were separated using a gradient from 92% A (0.1% FA in water) and 8% B (0.1% FA in acetonitrile) to 33% B, in 44 minutes at 300 nl min^{-1}, using a 250 mm × 75 μm i.d. 1.7 μM BEH C18, analytical column (Waters). Peptides were selected for fragmentation automatically by data dependant analysis. Data produced were searched using Mascot (Matrix Science UK), against the [*Uniprot*] database with taxonomy of [*mouse*] selected. Data were validated using Scaffold (Proteome Software, Portland, OR).

The Scaffold software (version 4.3.2, Proteome Software Inc.) was used to validate MS/MS based peptide and protein identifications and for relative quantification based on spectral counting. Peptide identifications were accepted if they could be established at > 95.0% probability by the Peptide Prophet algorithm with Scaffold delta-mass correction. Protein identifications were accepted if they could be established at > 99.0% probability and contained at least 2 identified peptides. Protein probabilities were assigned by the Protein Prophet algorithm. Proteins that contained similar peptides and could

not be differentiated based on MS/MS analysis alone were grouped to satisfy the principles of parsimony. Semi quantitative assessment of the protein amounts was conducted using normalized spectral counting, NSCs, provided by Scaffold Software. The mean value of NSCs obtained in the three experimental replicates for each protein was normalized to the protein MW and expressed as a relative quantity by applying the following equation:

$$MWNSC_k = \frac{\left(\frac{NSC}{MW}\right)_k}{\sum_{i=1}^{N}\left(\frac{NSC}{MW}\right)_i} \times 100 \quad (1)$$

where, MWNSCk is the percentage molecular weight normalized NSC for protein k and MW is the molecular weight in kDa for protein k. This equation takes into consideration the protein size and evaluates the contribution of each protein reflecting its relative protein abundance (RPA).

5.2. Statistical analysis

Statistical analysis of the data was performed using Graph Pad Prism software. Two-tailed unpaired student *t*-test was used and p values < 0.05 was considered significant.

Conflict of interest

The authors declare no competing financial interest.

Author contributions

Z.A. designed, planned and led the study, performed *in vivo* experiments, DOX encapsulation, DLS measurements, release studies, prepared figures and wrote the manuscript. M.H performed the recovery and purification of liposomes from plasma, TEM and protein corona characterization (SDS-PAGE, BCA assay and Mass Spectrometry). J.G prepared TSL formulation, DOX encapsulation and release studies. K·K. directed the experiments performed and project overall. Z.A, M.H and K.K wrote and reviewed the manuscript.

Acknowledgments

M.H and K.K. would like to acknowledge the Marie Curie Initial Training Network *PathChooser* (PITN-GA-2013-608373) for partially funding this research. The authors also wish to thank the staff in the Faculty of Life Sciences EM Facility for their assistance and the Wellcome Trust for equipment grant support to the EM Facility. In addition, Mass Spectrometry Facility staff at the University of Manchester for their assistance.

Appendix A. Supplementary data

Supplementary data to this article can be found online at https://doi.org/10.1016/j.jconrel.2018.02.038.

References

[1] M.B. Yatvin, J.N. Weinstein, W.H. Dennis, R. Blumenthal, Design of liposomes for enhanced local release of drugs by hyperthermia, Science 202 (1978) 1290–1293.
[2] Z.S. Al-Ahmady, K. Kostarelos, Chemical components for the design of temperature-responsive vesicles as cancer therapeutics, Chem. Rev. 116 (2016) 3883–3918.
[3] A.A. Manzoor, L.H. Lindner, C.D. Landon, J.Y. Park, A.J. Simnick, M.R. Dreher, S. Das, G. Hanna, W. Park, A. Chilkoti, G.A. Koning, T.L. ten Hagen, D. Needham, M.W. Dewhirst, Overcoming limitations in nanoparticle drug delivery: triggered, intravascular release to improve drug penetration into tumors, Cancer Res. 72 (2012) 5566–5575.
[4] Z.S. Al-Ahmady, O. Chaloin, K. Kostarelos, Monoclonal antibody-targeted, temperature-sensitive liposomes: in vivo tumor chemotherapeutics in combination with mild hyperthermia, J. Control. Release 196 (2014) 332–343.
[5] Z.S. Al-Ahmady, W.T. Al-Jamal, J.V. Bossche, T.T. Bui, A.F. Drake, A.J. Mason, K. Kostarelos, Lipid-peptide vesicle nanoscale hybrids for triggered drug release by mild hyperthermia in vitro and in vivo, ACS Nano 6 (2012) 9335–9346.
[6] W.T. Al-Jamal, Z.S. Al-Ahmady, K. Kostarelos, Pharmacokinetics & tissue distribution of temperature-sensitive liposomal doxorubicin in tumor-bearing mice triggered with mild hyperthermia, Biomaterials 33 (2012) 4608–4617.
[7] G. Kong, G. Anyarambhatla, W.P. Petros, R.D. Braun, O.M. Colvin, D. Needham, M.W. Dewhirst, Efficacy of liposomes and hyperthermia in a human tumor xenograft model: importance of triggered drug release, Cancer Res. 60 (2000) 6950–6957.
[8] Z.S. Al-Ahmady, C.L. Scudamore, K. Kostarelos, Triggered doxorubicin release in solid tumors from thermosensitive liposome-peptide hybrids: critical parameters and therapeutic efficacy, Int. J. Cancer 137 (2015) 731–743.
[9] C.D. Landon, J.-Y. Park, D. Needham, M.W. Dewhirst, Nanoscale drug delivery and hyperthermia: the materials design and preclinical and clinical testing of low temperature-sensitive liposomes used in combination with mild hyperthermia in the treatment of local cancer, Open Nanomed. J. 3 (2011) 38–64.
[10] D. Needham, J.-Y. Park, A.M. Wright, J. Tong, Materials characterization of the low temperature sensitive liposome (LTSL): effects of the lipid composition (lysolipid and dspe-peg2000) on the thermal transition and release of doxorubicin, Faraday Discuss. 161 (2013) 515–534.
[11] L. Li, T.L. Ten Hagen, M. Hossann, R. Suss, G.C. van Rhoon, A.M. Eggermont, D. Haemmerich, G.A. Koning, Mild hyperthermia triggered doxorubicin release from optimized stealth thermosensitive liposomes improves intratumoral drug delivery and efficacy, J. Control. Release 168 (2013) 142–150.
[12] L. Li, T.L.M. ten Hagen, D. Schipper, T.M. Wijnberg, G. Van Rhoon, A.M.M. Eggermont, L.H. Lindner, G.A. Koning, Triggered content release from optimized stealth thermosensitive liposomes using mild hyperthermia, J. Control. Release 143 (2010) 274–279.
[13] T. Hosokawa, M. Sami, Y. Kato, E. Hayakawa, Alteration in the temperature-dependent content release property of thermosensitive liposomes in plasma, Chem. Pharm. Bull. 51 (2003) 1227–1232.
[14] M.H. Gaber, K.L. Hong, S.K. Huang, D. Papahadjopoulos, Thermosensitive sterically stabilized liposomes - formulation and in-vitro studies on mechanism of doxorubicin release by bovine serum and human plasma, Pharm. Res. 12 (1995) 1407–1416.
[15] S. Unezaki, K. Maruyama, N. Takahashi, M. Koyama, T. Yuda, A. Suginaka, M. Iwatsuru, Enhanced delivery and antitumor-activity of doxorubicin using long-circulating thermosensitive liposomes containing amphipathic polyethylene-glycol in combination with local hyperthermia, Pharm. Res. 11 (1994) 1180–1185.
[16] T. Cedervall, I. Lynch, S. Lindman, T. Berggard, E. Thulin, H. Nilsson, K.A. Dawson, S. Linse, Understanding the nanoparticle-protein corona using methods to quantify exchange rates and affinities of proteins for nanoparticles, Proc. Natl. Acad. Sci. U. S. A. 104 (2007) 2050–2055.
[17] M. Hadjidemetriou, K. Kostarelos, Nanomedicine: evolution of the nanoparticle corona, Nat. Nanotechnol. 12 (2017) 288–290.
[18] M.P. Monopoli, A.S. Pitek, I. Lynch, K.A. Dawson, Formation and characterization of the nanoparticle-protein corona, Methods Mol. Biol. 1025 (2013) 137–155.
[19] S. Tenzer, D. Docter, J. Kuharev, A. Musyanovych, V. Fetz, R. Hecht, F. Schlenk, D. Fischer, K. Kiouptsi, C. Reinhardt, K. Landfester, H. Schild, M. Maskos, S.K. Knauer, R.H. Stauber, Rapid formation of plasma protein corona critically affects nanoparticle pathophysiology, Nat. Nanotechnol. 8 (2013) 772–781.
[20] S. Palchetti, V. Colapicchioni, L. Digiacomo, G. Caracciolo, D. Pozzi, A.L. Capriotti, G. La Barbera, A. Lagana, The protein corona of circulating PEGylated liposomes, Biochim. Biophys. Acta (2) (2016) 189–196.
[21] A. Chonn, S.C. Semple, P.R. Cullis, Association of blood proteins with large unilamellar liposomes in vivo. Relation to circulation lifetimes, J. Biol. Chem. 267 (1992) 18759–18765.
[22] T.M. Allen, C. Hansen, F. Martin, C. Redemann, A. Yau-Young, Liposomes containing synthetic lipid derivatives of poly(ethylene glycol) show prolonged circulation half-lives in vivo, Biochim. Biophys. Acta (1) (1991) 29–36.
[23] M. Hadjidemetriou, Z. Al-Ahmady, K. Kostarelos, Time-evolution of in vivo protein corona onto blood-circulating PEGylated liposomal doxorubicin (DOXIL) nanoparticles, Nano 8 (2016) 6948–6957.
[24] M. Hadjidemetriou, Z. Al-Ahmady, M. Mazza, R.F. Collins, K. Dawson, K. Kostarelos, In vivo biomolecule corona around blood-circulating, clinically used and antibody-targeted lipid bilayer nanoscale vesicles, ACS Nano 9 (2015) 8142–8156.
[25] S. Tenzer, D. Docter, J. Kuharev, A. Musyanovych, V. Fetz, R. Hecht, F. Schlenk, D. Fischer, K. Kiouptsi, C. Reinhardt, K. Landfester, H. Schild, M. Maskos, S.K. Knauer, R.H. Stauber, Rapid formation of plasma protein corona critically affects nanoparticle pathophysiology, Nat. Nanotechnol. 8 (2013) 772–781.
[26] D. Pozzi, G. Caracciolo, L. Digiacomo, V. Colapicchioni, S. Palchetti, A.L. Capriotti, C. Cavaliere, R. Zenezini Chiozzi, A. Puglisi, A. Lagana, The biomolecular corona of nanoparticles in circulating biological media, Nano 7 (2015) 13958–13966.
[27] C. Ge, J. Du, L. Zhao, L. Wang, Y. Liu, D. Li, Y. Yang, R. Zhou, Y. Zhao, Z. Chai, C. Chen, Binding of blood proteins to carbon nanotubes reduces cytotoxicity, Proc. Natl. Acad. Sci. U. S. A. 108 (2011) 16968–16973.
[28] A. Salvati, A.S. Pitek, M.P. Monopoli, K. Prapainop, F.B. Bombelli, D.R. Hristov, P.M. Kelly, C. Aberg, E. Mahon, K.A. Dawson, Transferrin-functionalized nanoparticles lose their targeting capabilities when a biomolecule corona adsorbs on the surface, Nat. Nanotechnol. 8 (2013) 137–143.
[29] V. Mirshafiee, M. Mahmoudi, K. Lou, J. Cheng, M.L. Kraft, Protein corona significantly reduces active targeting yield, Chem. Commun. 49 (2013) 2557–2559.
[30] Q. Dai, C. Walkey, W.C. Chan, Polyethylene glycol backfilling mitigates the negative impact of the protein corona on nanoparticle cell targeting, Angew. Chem. Int. Ed. Eng. 53 (2014) 5093–5096.

[31] A. Pourjavadi, Z.M. Tehrani, N. Mahmoudi, The effect of protein corona on doxorubicin release from the magnetic mesoporous silica nanoparticles with polyethylene glycol coating, J. Nanopart. Res. 17 (2015).
[32] R. Garcia-Alvarez, M. Hadjidemetriou, A. Sanchez-Iglesias, L.M. Liz-Marzan, K. Kostarelos, In vivo formation of protein corona on gold nanoparticles. The effect of their size and shape, Nano 10 (2018) 1256–1264.
[33] M.H. Gaber, Effect of bovine serum on the phase transition temperature of cholesterol-containing liposomes, J. Microencapsul. 15 (1998) 207–214.
[34] J.K. Mills, D. Needham, Lysolipid incorporation in dipalmitoylphosphatidylcholine bilayer membranes enhances the ion permeability and drug release rates at the membrane phase transition, Biochim. Biophys. Acta Biomembr. 1716 (2005) 77–96.
[35] D. Needham, G. Anyarambhatla, G. Kong, M.W. Dewhirst, A new temperature-sensitive liposome for use with mild hyperthermia: characterization and testing in a human tumor xenograft model, Cancer Res. 60 (2000) 1197–1201.
[36] B. Banno, L.M. Ickenstein, G.N. Chiu, M.B. Bally, J. Thewalt, E. Brief, E.K. Wasan, The functional roles of poly(ethylene glycol)-lipid and lysolipid in the drug retention and release from lysolipid-containing thermosensitive liposomes in vitro and in vivo, J. Pharm. Sci. 99 (2010) 2295–2308.
[37] G. Caracciolo, D. Pozzi, A.L. Capriotti, C. Cavaliere, S. Piovesana, H. Amenitsch, A. Lagana, Lipid composition: a "key factor" for the rational manipulation of the liposome-protein corona by liposome design, RSC Adv. 5 (2015) 5967–5975.
[38] M. Mahmoudi, A.M. Abdelmonem, S. Behzadi, J.H. Clement, S. Dutz, M.R. Ejtehadi, R. Hartmann, K. Kantner, U. Linne, P. Maffre, S. Metzler, M.K. Moghadam, C. Pfeiffer, M. Rezaei, P. Ruiz-Lozano, V. Serpooshan, M.A. Shokrgozar, G.U. Nienhaus, W.J. Parak, Temperature: the "ignored" factor at the NanoBio interface, ACS Nano 7 (2013) 6555–6562.
[39] M. Hossann, Z. Syunyaeva, R. Schmidt, A. Zengerle, H. Eibl, R.D. Issels, L.H. Lindner, Proteins and cholesterol lipid vesicles are mediators of drug release from thermosensitive liposomes, J. Control. Release 162 (2012) 400–406.
[40] M.W. Dewhirst, C.D. Landon, C.L. Hofmann, P.R. Stauffer, Novel approaches to treatment of hepatocellular carcinoma and hepatic metastases using thermal ablation and thermosensitive liposomes, Surg. Oncol. Clin. N. Am. 22 (2013) 545–561.
[41] ClinicalTrials.gov, A Study of ThermoDox™ in Combination with Radiofrequency Ablation (RFA) in Primary and Metastatic Tumors of the Liver (NCT00441376), (2015).
[42] ClinicalTrials.gov, Phase 1/2 Study of ThermoDox with Approved Hyperthermia in Treatment of Breast Cancer Recurrence at the Chest Wall, (2015).
[43] M. Hossann, M. Wiggenhorn, A. Schwerdt, K. Wachholz, N. Teichert, H. Eibl, R.D. Issels, L.H. Lindner, In vitro stability and content release properties of phosphatidylglyceroglycerol containing thermosensitive liposomes, Biochim. Biophys. Acta Biomembr. 1768 (2007) 2491–2499.
[44] S.M. Park, M.S. Kim, S.J. Park, E.S. Park, K.S. Choi, Y.S. Kim, H.R. Kim, Novel temperature-triggered liposome with high stability: formulation, in vitro evaluation, and in vivo study combined with high-intensity focused ultrasound (HIFU), J. Control. Release 170 (2013) 373–379.
[45] T. Tagami, M.J. Ernsting, S.-D. Li, Optimization of a novel and improved thermosensitive liposome formulated with DPPC and a Brij surfactant using a robust in vitro system, J. Control. Release 154 (2011) 290–297.
[46] W.J. Lokerse, E.C. Kneepkens, T.L. Ten Hagen, A.M. Eggermont, H. Grull, G.A. Koning, In depth study on thermosensitive liposomes: optimizing formulations for tumor specific therapy and in vitro to in vivo relations, Biomaterials 82 (2016) 138–150.
[47] M. de Smet, S. Langereis, S. van den Bosch, H. Gruell, Temperature-sensitive liposomes for doxorubicin delivery under MRI guidance, J. Control. Release 143 (2010) 120–127.
[48] G. Kong, M.W. Dewhirst, Hyperthermia and liposomes, Int. J. Hyperth. 15 (1999) 345–370.
[49] Q. Peng, X.Q. Wei, Q. Yang, S. Zhang, T. Zhang, X.R. Shao, X.X. Cai, Z.R. Zhang, Y.F. Lin, Enhanced biostability of nanoparticle-based drug delivery systems by albumin corona, Nanomedicine 10 (2015) 205–214.
[50] S. Behzadi, V. Serpooshan, R. Sakhtianchi, B. Muller, K. Landfester, D. Crespy, M. Mahmoudi, Protein corona change the drug release profile of nanocarriers: the “overlooked” factor at the nanobio interface, Colloids Surf. B 123 (2014) 143–149.
[51] A. Cifuentes-Rius, H. de Puig, J.C. Kah, S. Borros, K. Hamad-Schifferli, Optimizing the properties of the protein corona surrounding nanoparticles for tuning payload release, ACS Nano 7 (2013) 10066–10074.
[52] J.C. Kah, J. Chen, A. Zubieta, K. Hamad-Schifferli, Exploiting the protein corona around gold nanorods for loading and triggered release, ACS Nano 6 (2012) 6730–6740.
[53] Celsion.com, Celsion Corporation Announces Updated Overall Survival Data from HEAT Study of ThermoDox® in Primary Liver Cancer, (2015).
[54] D. Needham, Chapter 12 - reverse engineering of the low temperature-sensitive liposome (ltsl) for treating cancer, in: K. Park (Ed.), Biomaterials for Cancer Therapeutics, Woodhead Publishing, 2013, pp. 270–353e.